

Rebecca Stein-Wexler and Mahesh M. Thapa

Contents

1	Juvenile Idiopathic Arthritis	652
1.1	Enthesitis-Related Arthritis (ERA).....	666
2	Hemophilic Arthropathy	668
3	Pigmented Villonodular Synovitis	672
	References	677

Abstract

Imaging plays a key role in the evaluation of patients with known or suspected arthritis. Following clinical and laboratory assessment, radiography is the traditional imaging starting point. Other potential modalities include ultrasound, computed tomography, nuclear medicine, and magnetic resonance imaging. This chapter will present the following conditions: juvenile idiopathic arthritis (JIA) along with the enthesitis-related arthritis (ERA) subtype, hemophilia, and pigmented villonodular synovitis (PVNS). Synovial chondromatosis and dermatomyositis are discussed in Chaps. 12 and 24, respectively.

The child with chronic joint pain often presents a diagnostic challenge. Radiographs constitute the initial imaging modality, but in children with arthritis, these studies are usually normal until relatively late in the disease—or they demonstrate only nonspecific soft tissue swelling and joint fluid. Only after chronic inflammation has destroyed the thick cartilage that covers the bone do findings such as joint space narrowing, osseous erosions, ankylosis, and growth disturbance become apparent. Diagnosis therefore often rests on clinical factors along with advanced imaging, typically gadolinium-enhanced magnetic resonance imaging (MRI) although Doppler ultrasound (US) may also contribute useful information.

R. Stein-Wexler, MD (✉)
 Department of Radiology,
 University of California Davis Medical
 Center and UC Davis Children's Hospital,
 4860 Y Street, Suite 3100, Sacramento, CA 95817, USA

Department of Diagnostic Imaging, Shriners Hospitals
 for Children Northern California,
 Sacramento, CA 95817, USA
 e-mail: rebecca.steinwexler@ucdmc.ucdavis.edu

M.M. Thapa, MD
 Department of Radiology, Seattle Children's Hospital,
 4800 Sand Point Way NE, Seattle, WA 98105, USA
 e-mail: thapamd@uw.edu

1 Juvenile Idiopathic Arthritis

Juvenile idiopathic arthritis (JIA) is the most common chronic rheumatic disease of childhood and encompasses all idiopathic arthritides that present before age 16 years and last at least 6 weeks. The disorder is further classified according to the number of joints involved (up to four being “oligoarticular”), the presence of systemic disease, and the results of serologic tests for rheumatic factor. Prevalence is 1 per 1,000 children [1], and the disease is most common in girls. Patients present with joint pain and swelling and sometimes with extraskeletal findings as well.

Etiology is multifactorial, with both environmental and genetic factors playing a role. The disease appears to develop when a genetically predisposed child mounts a particular immunological response to an infectious process. Pannus and inflammation develop within the synovium

after an antigen-antibody cross-reaction [2]. Initial synovitis progresses to synovial hyperplasia and formation of highly cellular inflammatory pannus. This eventually erodes the overlying cartilage and bone and causes articular destruction, ankylosis, and growth disturbance.

The term JIA replaces older terminology, such as “juvenile chronic arthritis” and “juvenile rheumatoid arthritis.” The newer term, with its subtypes, facilitates more accurate identification of homogeneous groups of children with distinct clinical features. The International League of Associations for Rheumatology (ILAR) identifies eight distinct subtypes of JIA [3], and this classification system will almost certainly undergo further refinement (Table 20.1).

The most common JIA subtype, “oligoarticular,” affects no more than four joints during the first 6 months of presentation; it usually affects the knees and/or ankles, as well as the wrists and elbows, of girls less than 6 years old [1]. Up to

Table 20.1 ILAR classification of juvenile idiopathic arthritis

Arthritis	Inclusionary criteria
Systemic arthritis	Arthritis in at least one joint 2 weeks' fever consecutive at least 3 days Rash, generalized lymphadenopathy, hepatomegaly/splenomegaly, or serositis
Oligoarthritis (persistent)	Arthritis of 1–4 joints during the first 6 months Never involves more than 4 joints
Oligoarthritis (extended)	Arthritis of 1–4 joints during the first 6 months Eventually affects at least 5 joints
Polyarthritis (RF negative)	Arthritis of more than 5 joints during the first 6 months RF test negative
Polyarthritis (RF positive)	Arthritis of more than 5 joints during the first 6 months RF test positive (at least twice, during the first 6 months)
Psoriatic arthritis	Arthritis and psoriasis Or arthritis and at least 2 in first-degree relative: Dactylitis, nail pitting, psoriasis
Enthesitis-related arthritis	Arthritis and enthesitis, with Sacroiliac joint tenderness and/or lumbosacral pain HLA-B27 antigen Male over 6-year-old Acute anterior uveitis First-degree relative with ankylosing spondylitis, enthesitis-related arthritis, sacroiliitis with inflammatory bowel disease, Reiter syndrome, or acute anterior uveitis
Undifferentiated arthritis	Arthritis that fulfills two or more of these categories or that fails to fall into one of these categories

Adapted from Wallace and Levinson [4]

30 % of these children also have iridocyclitis. "Polyarticular" arthritis presents with involvement of at least five joints within 6 months of presentation and is usually symmetric, involving the wrists, hands, and feet. Results of serologic testing allow further categorization: RF-positive cases typically occur in adolescent girls, and like rheumatoid arthritis in adults, the disease affects the small joints of the hands. RF-negative cases, which have a broad variety of manifestations, occur throughout childhood.

Arthritis is categorized as systemic if at least one joint is affected and if accompanied or recently preceded by at least 2 weeks of fever (consecutive for at least 3 days), a transitory rash, hepatomegaly, splenomegaly, lymphadenopathy, or serositis. Classic polyarticular and symmetric symptoms generally occur late in the course of disease. Systemic JIA may be life-threatening in a small subset of patients who develop pancytopenia, disseminated intravascular coagulation, and multiorgan failure ("macrophage activation syndrome").

Psoriatic arthritis and enthesitis-related arthritis (ERA) subtypes are based on the presence of dactylitis, psoriasis, symptoms related to the sacroiliac joints or lower back, presence of human leukocyte antigen (HLA)-B27, and additional findings. Juvenile psoriatic arthritis affects large or small joints, and joint findings may precede development of skin abnormalities. ERA (formerly termed juvenile spondyloarthritis) is unusual among the subtypes of JIA in that the hip is often affected. This disease tends to affect sites of tendinous and ligamentous insertion at the pelvis, knee, and calcaneus. Axial involvement is rare in children under 10 years of age, although the spine and sacroiliac joints may be affected in older children (see following section for further discussion of Sect. 1.1). Undifferentiated JIA encompasses cases with none of these features or with features that are present in at least two different subtypes.

Disease usually becomes inactive with anti-inflammatory medication. However, in many patients, disease progresses unabated, regardless of treatment. Between 28 and 55 % of patients develop cartilage or bone erosions,

often leading to joint irregularity, within 7 years of initial diagnosis [4]. Ankylosis, most common in the carpal and tarsal bones as well as the cervical spine, may develop within 3–5 years of disease onset.

Imaging (Table 20.1)

General Considerations. Radiographs are often initially normal, but in the early phase there may be nonspecific consequences of hypervascularity and inflammation, including joint effusion, soft tissue swelling, epiphyseal widening, and periarticular osteopenia. This is partly because in the pediatric skeleton thick cartilage protects bone, so erosive change is encountered only with advanced disease. In addition, the synovial hypertrophy and cartilaginous changes typical of early JIA are radiographically occult. However, radiographs performed early in the course of disease do both allow exclusion of other causes of pain and establish a baseline. US and MRI are able to demonstrate early findings of synovial hypertrophy and hyperemia.

During the intermediate phase, cartilage destruction results in joint space narrowing, cortical erosions, and epiphyseal overgrowth; these findings are demonstrable on both radiographs and MRI and to a lesser extent US. Finally, ankylosis, muscle atrophy, growth disturbance, angular deformity at the joints, and contractures may be seen with late disease.

During active disease, clinical examination generally provides adequate assessment of articular synovitis. US and MRI are, however, useful for early staging and for monitoring response to therapy. Indeed, techniques such as T2 mapping may demonstrate progressive cartilage deterioration even when clinical findings are stable [5]. Numerous attempts have been made to develop radiographic scoring systems, none of which have been widely accepted [6, 7]. Radiographs therefore do not play an important role in monitoring progression, but they are important for evaluating deformities and growth abnormalities.

Radiographic Findings. Radiographs may demonstrate joint effusions early in JIA, especially at the knee (Fig. 20.1) The small joints of the hands and feet may show fusiform soft tis-



Fig. 20.1 Knee effusion in a 3-year-old boy with polyarticular juvenile idiopathic arthritis (JIA), symptomatic since age 1 year. There are also growth arrest lines and juxta-articular osteopenia. Findings were bilaterally symmetric (Same patient as Fig. 20.4) (Image copyright Shriners Hospital for Children Northern California)

sue swelling, especially common with psoriatic arthritis. US and MRI are more sensitive for evaluation of the small joints than are radiographs.

Osteopenia is another relatively early finding (Fig. 20.2). In the acute setting, this results from juxta-articular hyperemia and resultant trabecular resorption, whereas in chronic disease it is more generalized and results from steroid use and disuse atrophy.

Periostitis occurs at any stage of disease and in any long bone but is most common in the short tubular bones of the hands and feet (Fig. 20.3). This usually develops at para-articular locations, due to inflammation of the joint capsule and tendinous insertions. Bones may enlarge and become square as a result (especially common with psoriatic arthritis) (Fig. 20.4).

Erosions are evident relatively late, after thick protective cartilage has been destroyed by prolonged synovial proliferation (Fig. 20.5). Although erosions may occur anywhere along



Fig. 20.2 Erosions and osteopenia in a 10-year-old girl with seronegative polyarticular JIA. In addition to the carpal erosions and juxta-articular demineralization/soft tissue swelling, there are flexion deformities at the third through fifth proximal interphalangeal (PIP) joints (Image copyright Shriners Hospital for Children Northern California)

the articular surface, they are most common at locations where there is less cartilage—insertion sites of intraosseous ligaments and synovial reflections. Radiographs show decreased joint space due to cartilage loss before erosions become apparent, but they are relatively insensitive for showing trabecular bone loss [8]. In patients with systemic JIA, joint space narrowing and erosions may be found relatively early in the course of disease [9].

Growth disturbance, a relatively late finding, is both more common and more severe in children with early onset of disease. It may be generalized, resulting from chronic disease and long-term steroid use. Alternatively, localized growth disturbance may result from periarticular inflammation and localized hyperemia, which lead to early growth acceleration and subsequent epiphyseal enlargement as well as early physeal closure and accelerated maturation. This accounts



Fig. 20.3 Periostitis in a 15-year-old girl with psoriatic JIA. (a) Marked soft tissue swelling, moderate joint space narrowing, and erosions at the PIP joint of the right fourth digit. Periosteal reaction along the proximal phalanx. (b) Eight months later, after methotrexate therapy, findings have improved (Images copyright Shriners Hospital for Children Northern California)

for the typical appearance at the knee (Figs. 20.6 and 20.7): ballooned epiphyses, wide intercondylar notch, and squared inferior patella, which may in turn lead to subluxation. Although hyperemia leads to initial growth acceleration and longitudinal overgrowth, premature bone maturation and physeal fusion/epiphyseal destruction may eventually cause decreased limb length. A similar process takes place in the carpal and tarsal bones, which may demonstrate premature ossification and then osseous coalition (Fig. 20.8).



Fig. 20.4 Squaring of phalanges in a 3-year-old boy with polyarticular JIA. Findings are most striking in the proximal and middle phalanges, where periostitis causes thickening of phalanges. Diffuse soft tissue swelling (Same patient as Fig. 20.1) (Image copyright Shriners Hospital for Children Northern California)



Fig. 20.5 Disease progression in a teenage girl with systemic JIA. (a) At age 15 years, there are small femoral head erosions and uniform joint space narrowing on the left, whereas the right is almost normal. (b) Two years later, the joint space on the left is barely evident, and there

are more acetabular and femoral head erosions as well as sclerosis. The right femoral head is developing erosions (Images copyright Shriners Hospital for Children Northern California)



Fig. 20.6 Knee deformity in chronic JIA. Epiphyseal squaring, femoral notch enlargement, joint space narrowing, and subchondral cysts are typical of long-standing disease. Dislocated patella (Image copyright Shriners Hospital for Children Northern California)

Growth disturbance is also common in the mandible (see discussion below).

Ankylosis (Fig. 20.9), erosions, synovial hypertrophy, effusions, and muscle imbalance may cause abnormal stress at the joints and lead to flexion and extension deformities as well as joint subluxation and dislocation (see subsequent paragraph). The knee may develop varus or valgus deformity, in part due to asymmetric epiphyseal overgrowth (see Fig. 20.7). This may contribute to deformity at the hip, including enlargement of the femoral head, acetabular protrusion, coxa vara, and hip subluxation. A similar process may occur in the upper extremities, with asymmetric epiphyseal enlargement causing deformity at the elbow and shoulder (Figs. 20.10 and 20.11).

Deformities at the hand and wrist are most common with polyarticular JIA. These include such finger deformities as flexion at the proximal interphalangeal (PIP) and distal interphalangeal (DIP) joints, Boutonniere deformity (flexion at PIP with hyperextension at DIP) (Fig. 20.12), and swan neck deformity (extension at PIP and

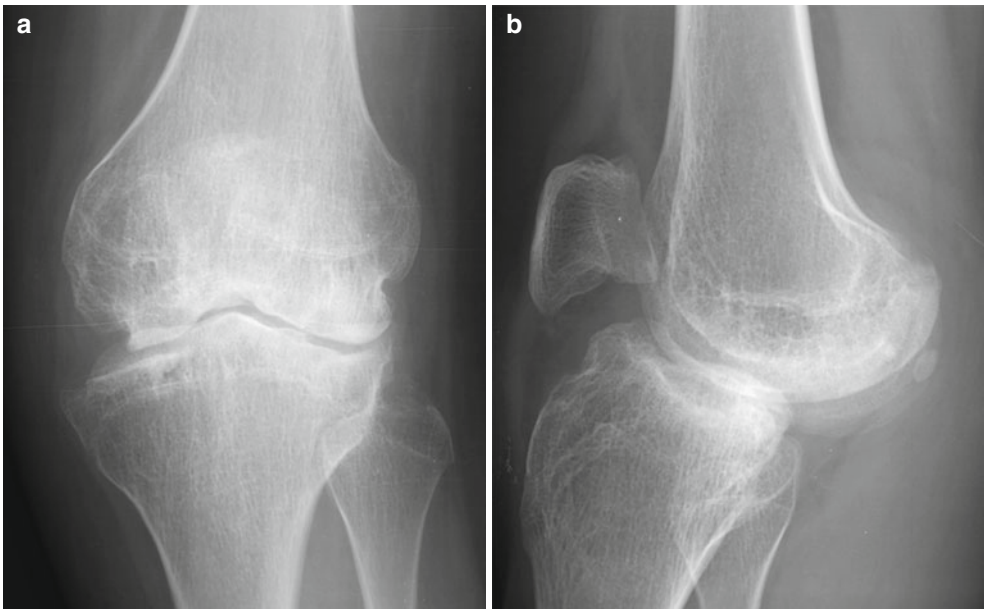


Fig. 20.7 Knee deformity and subluxation in an 18-year-old female with JIA. (a) Epiphyseal enlargement and asymmetric growth, joint space narrowing, subchondral cysts, and valgus deformity are characteristic of long-

standing disease. (b) Squaring of the patella and subluxation at the tibiofemoral joint. Findings were bilaterally symmetric (Same patient as Fig. 20.17) (Images copyright Shriners Hospital for Children Northern California)

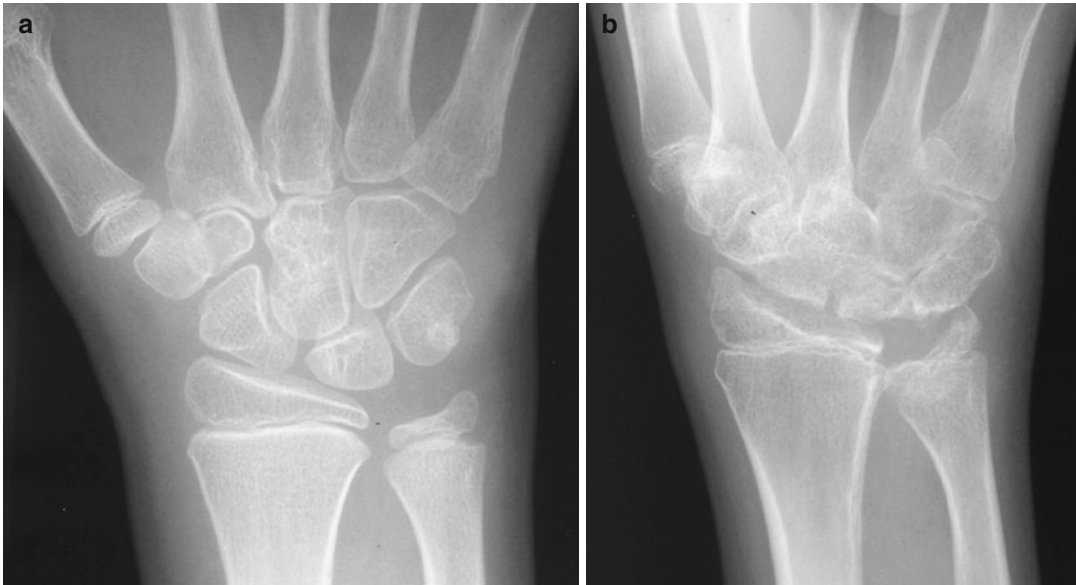
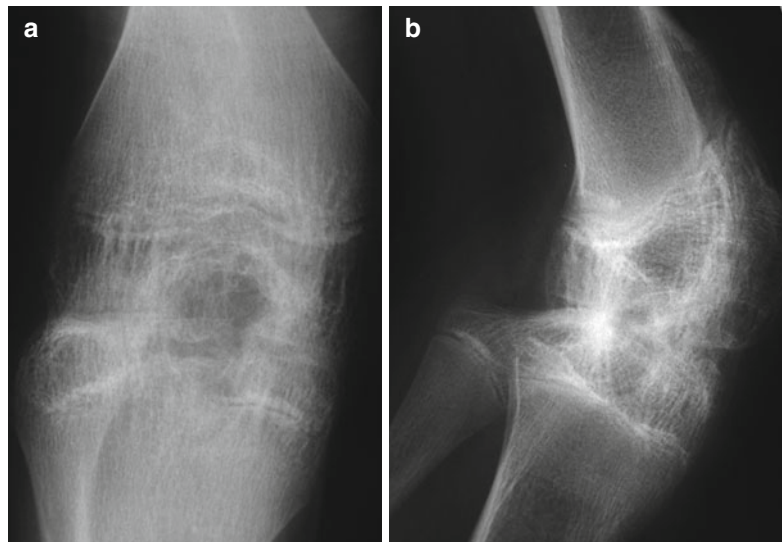


Fig. 20.8 Progression of carpal pathology in a girl with polyarticular JIA. (a) Slight intercarpal joint space narrowing at age 9 years. (b) At age 15 years, there is marked intercarpal narrowing, along with erosions and developing

ankylosis. Note erosions and deformity of the distal radius and ulna. The gap at the radiocarpal articulation is likely due to hypertrophic pannus (Images copyright Shriners Hospital for Children Northern California)

Fig. 20.9 Ankylosis at the knee in late-stage polyarticular JIA. (a, b) Growth plates are still open, and the femoral notch is enlarged (Images copyright Shriners Hospital for Children Northern California)



flexion at DIP). Ligamentous laxity and sometimes mass-like hypertrophied synovium may lead to carpal subluxation or dislocation, especially common at the hamate. The wrist may deviate in a radial direction [7].

Patients with the psoriatic or enthesitis-related subtypes may demonstrate overgrowth and

inflammation of a digit (dactylitis) (Fig. 20.13). ERA may manifest with thickening of tendons and ligaments, showing wispy periostitis along their osseous attachments.

Ultrasound. Both US and MRI may be used for early assessment of the disease process (Fig. 20.14). US depicts the severity of disease

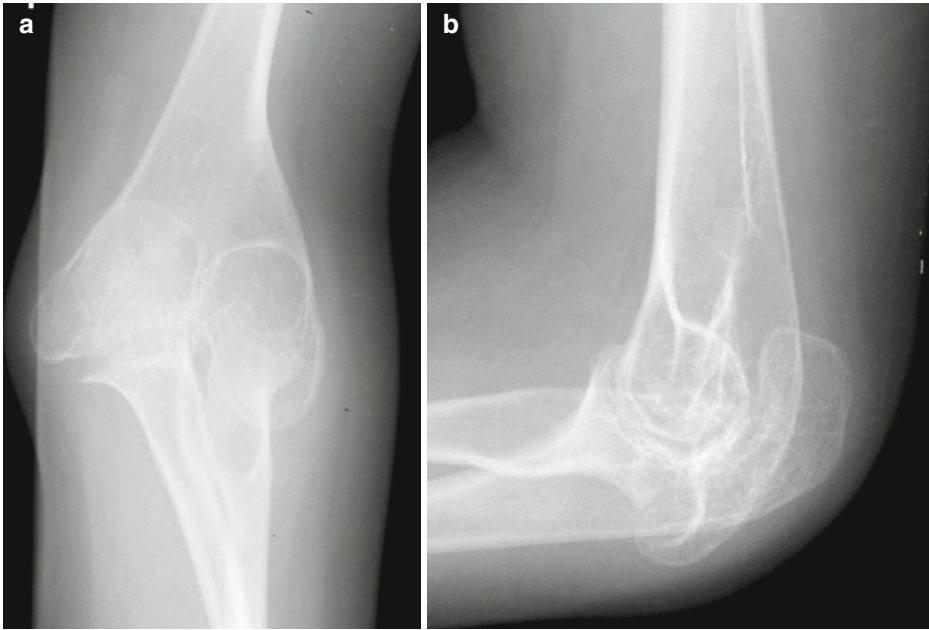


Fig. 20.10 Elbow deformity in a 13-year-old girl with polyarticular JIA. (a, b) Osteopenia, epiphyseal enlargement, and joint space narrowing (Images copyright Shriners Hospital for Children Northern California)



Fig. 20.11 Shoulder deformity in a 17-year-old girl with polyarticular JIA. There are erosions and deformity of the humeral head (Image copyright Shriners Hospital for Children Northern California)



Fig. 20.12 Boutonniere deformity in a 19-year-old male with JIA (Image copyright Shriners Hospital for Children Northern California)

by allowing assessment of joint effusions, synovial thickening, cartilage destruction/thinning, associated synovial cysts, erosions, and tenosynovitis (Figs. 20.15 and 20.16). It may identify clinically occult knee effusions as well as sub-clinical synovitis in multiple joints [10, 11].

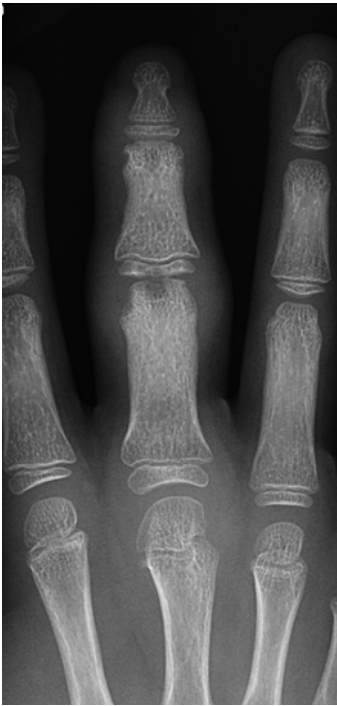


Fig. 20.13 Sausage digit in a child with psoriatic arthritis. There is soft tissue swelling at the PIP and DIP joints, along with central erosions. Increased width of the affected phalanges results in brachydactyly (Courtesy of J. Herman Kan)

Later on, it may identify enthesitis, inflammation of tendons or ligaments where they insert into the bone (most common at the calcaneal insertion of the Achilles tendon). US is especially useful for evaluating the joints of the hand and feet. It may be employed to guide joint aspiration or therapeutic injection, and it helps assess response to intra-articular treatment [7].

Synovial proliferation appears as hypoechoic, irregular synovial membrane thickening, easily distinguishable from joint fluid (see Chap. 22). With cartilage involvement, the normal smooth contour of hypoechoic cartilage is altered, and the typically sharp margins become blurred and obliterated [10]. Erosions appear as a break in the cortex that measures at least 2 mm; the floor is irregular, and adjacent marrow demonstrates acoustic enhancement [12].

If power Doppler demonstrates hypervascular pannus, disease is considered active (see Fig. 20.14). Serial US may then be used to monitor

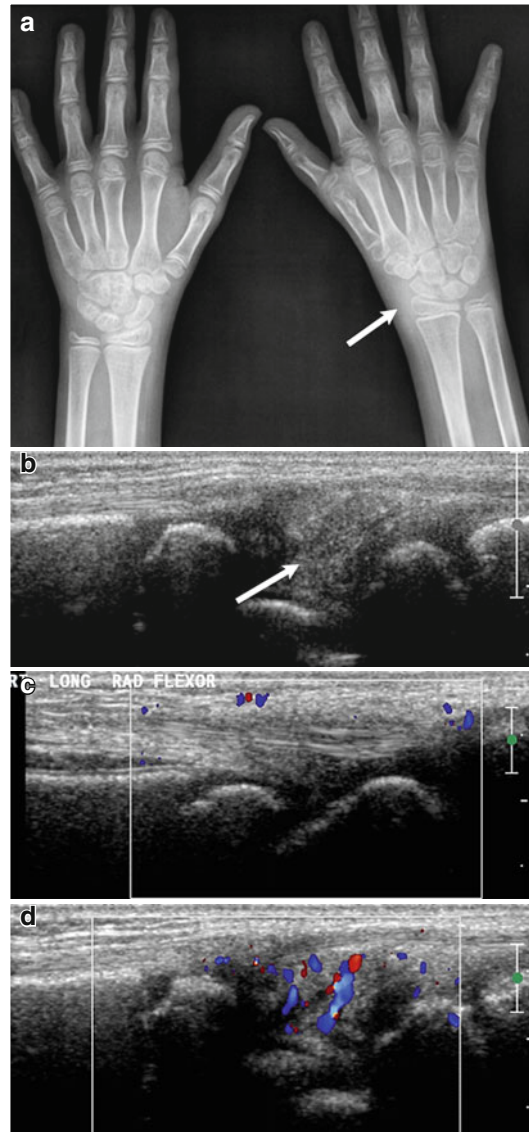


Fig. 20.14 New onset of significant left thenar atrophy, swelling around the wrist, and limited motion in a 7-year-old girl who subsequently received a diagnosis of antinuclear antibody (ANA)- and rheumatoid factor (RF)-negative JIA. (a) There is minimal lateral soft tissue swelling (*arrow*). (b) Longitudinal ultrasound (US) of the radial aspect of the wrist shows thickened, echogenic synovial tissue (*arrow*). (c) Color Doppler of the unaffected wrist shows normal flow (for comparison). (d) The affected side is hyperemic (Reprinted from Miller and Doria [37], with kind permission from Springer Science + Business Media) (Image courtesy of Andrea Doria)

disease activity and demonstrate response to therapy, showing decreased thickness and vascularity of the synovium, as well as a decrease in joint fluid

Fig. 20.15 Tenosynovitis in a 7-year-old girl with JIA. (a) Longitudinal US shows pannus along the tendon sheath (*arrow*). (b) Axial short tau inversion recovery (STIR) image of the wrist shows fluid (*arrow*) and pannus (*arrowheads*) surrounding thickened extensor digitorum tendons (Courtesy of J. Herman Kan)

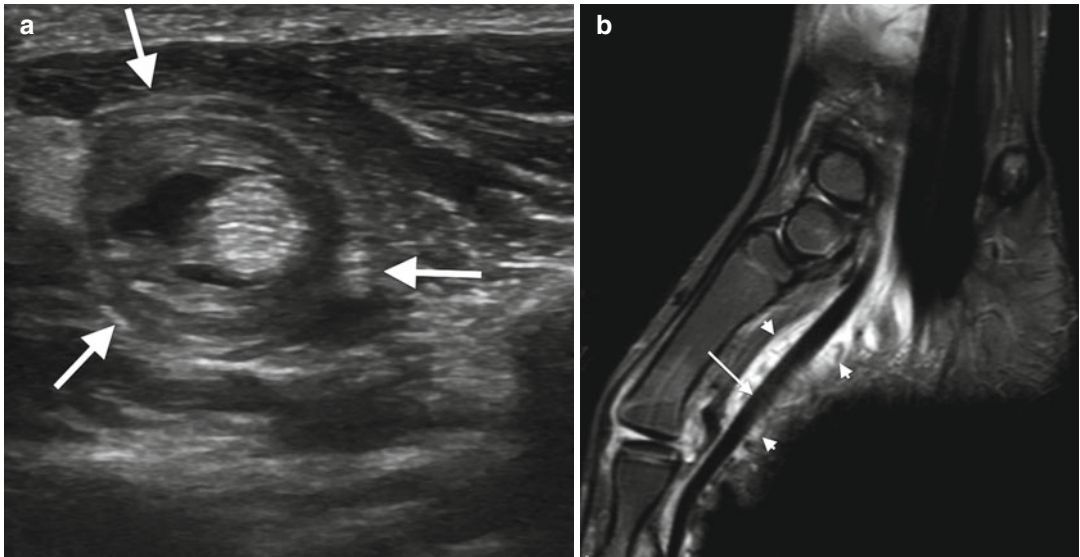
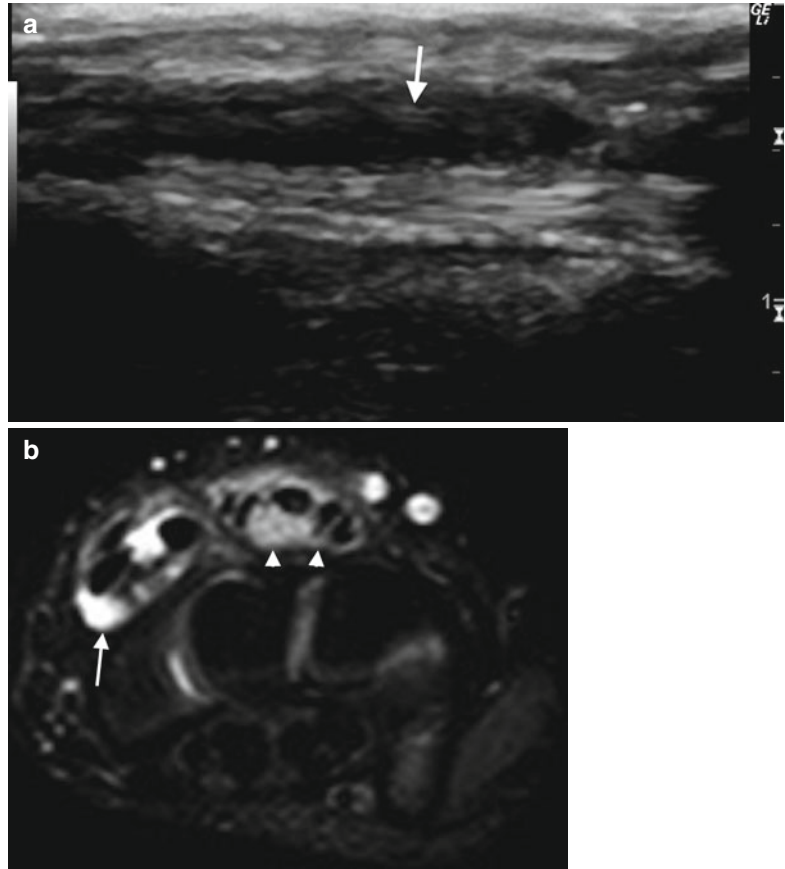


Fig. 20.16 Tenosynovitis in an 11-year-old boy. (a) Axial US of the flexor pollicis longus demonstrates circumferential thickening of the tendon sheath (*arrows*) and tenosynovial fluid. (b) Sagittal STIR image shows exten-

sive tenosynovitis of the flexor pollicis longus. The tendon is thickened and mildly hyperintense (*arrow*), and there is surrounding fluid and soft tissue edema (*arrowheads*). Note fluid in the MTP joint (Courtesy of J. Herman Kan)

[13]. However, US provides only limited visualization of some joints (such as the sacroiliac and temporomandibular joints), and a narrow acoustic window may preclude complete assessment of large joints. The efficacy of US is also limited by difficulty in positioning and examining children whose joints are swollen and painful.

Magnetic Resonance Imaging. MRI offers optimal assessment of joint disease in JIA, and contrast-enhanced MRI is the most sensitive technique for detecting synovitis, demonstrating pathology even before the physical exam becomes abnormal. It is superior to US in depicting early inflammation and synovitis, as well as in evaluation of the cartilage. MRI readily shows marrow edema, which predicts future erosions [14]. It also accurately evaluates the late manifestations of the disease, including erosions, joint space loss, and ligamentous involvement (Figs. 20.17, 20.18, and 20.19) [7, 13, 15]. MRI thus plays an important role in determining prognosis.

Joint effusion and acute synovitis constitute the earliest MRI manifestations in JIA (Fig. 20.20) [16]. Joint fluid and thickened synovium appear similar on conventional spin echo images. However, heavily T2-weighted (T2-W) images and fast spin echo (FSE) tech-

niques differentiate hyperintense joint fluid from relatively hypointense synovium [13]. Normal synovium (Fig. 20.21) is at most 2 mm thick and appears hypointense on T1-weighted (T1-W) and T2-W sequences. Abnormal synovium appears as a thick, irregular, wavy layer that is hypo- to isointense on T1-W and hyperintense on T2-W sequences (Fig. 20.22). T2-W sequences may delineate frond-like pannus, formed when progressive inflammation leads to synovial proliferation (Fig. 20.23). Hypertrophic synovium may slough and undergo fibrinoid necrosis, forming intra-articular loose bodies (“rice bodies”), readily apparent on heavily T2-W images (Fig. 20.24). These loose bodies preclude the use of intra-articular steroids.

The presence of enhancement also helps differentiate between normal and abnormal synovium. Normal synovium may show minimal enhancement on T1-W fat-suppressed (FS) imaging, but avid early enhancement indicates the presence of synovitis (see Fig. 20.24). Intense enhancement also helps differentiate thickened synovium from simple joint fluid (scanning should be performed within 5–10 min of administration of gadolinium, as contrast eventually diffuses into the joint). Administration of gadolinium is essential for distinguishing active, hypervascu-

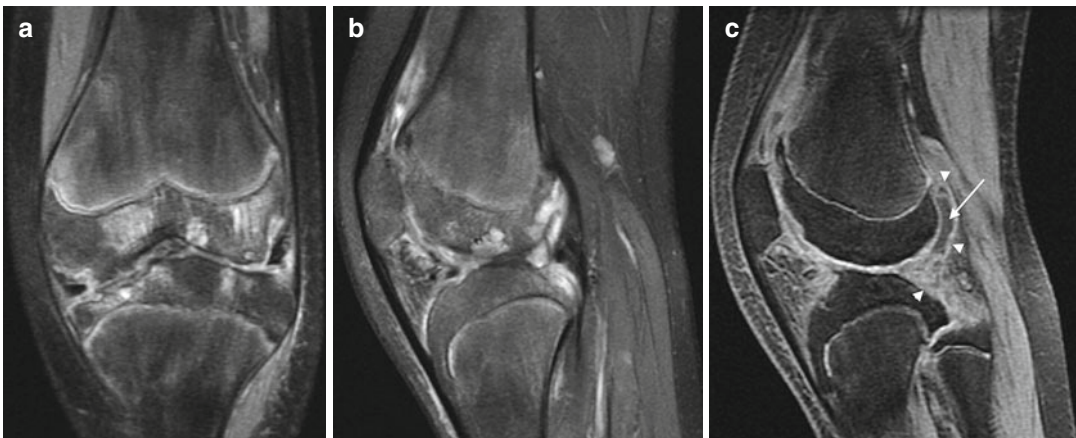


Fig. 20.17 JIA in a 14-year-old girl with polyarticular disease. (a) Coronal proton density (PD) FS image of the knee shows cartilage destruction with joint space narrowing, epiphyseal marrow edema, subcortical erosions and cysts, and deformity. Central menisci are compressed. (b) On sagittal T2-W image, synovial inflammation and joint

fluid result in diffuse hyperintensity (arrows). (c) Enhancement on sagittal spoiled gradient (SPGR) gadolinium-enhanced image differentiates joint fluid (arrow) from the synovium (arrowheads) (same patient as Fig. 20.7)

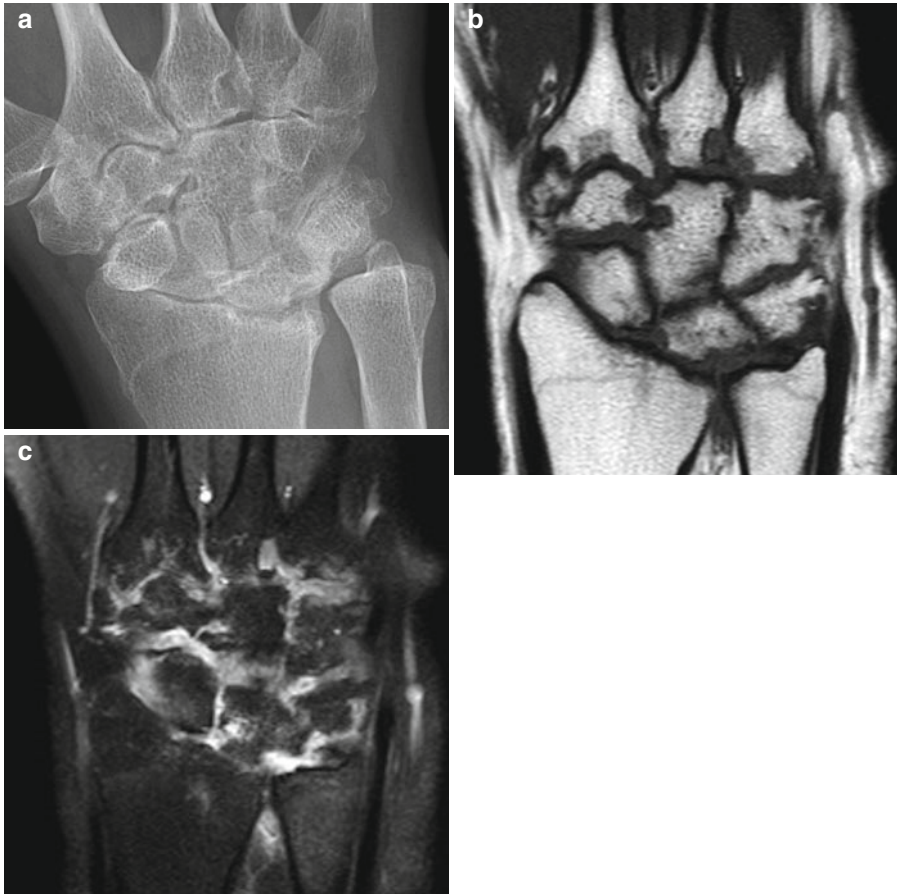


Fig. 20.18 Late manifestations of JIA in an 18-year-old female. (a) Radiograph shows extensive erosions, joint space narrowing, and ulnar overgrowth. (b) Coronal T1-W image better delineates multiple erosions. (c) Coronal

T1-W FS gadolinium-enhanced image shows enhancing synovium throughout all carpal joint spaces and extending into the erosions (Courtesy of J. Herman Kan)

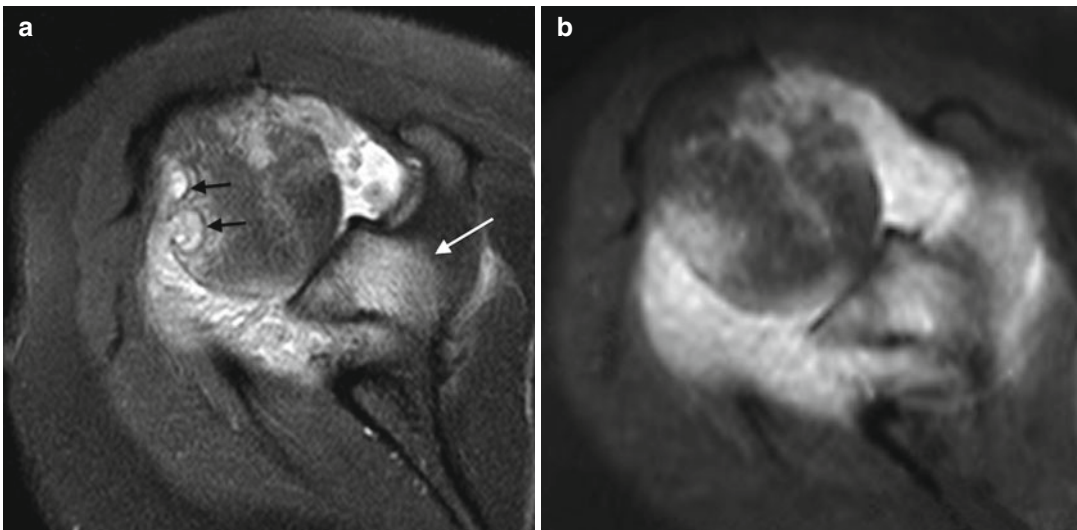


Fig. 20.19 Advanced JIA in a 16-year-old girl. (a) Axial T2-W image of the shoulder shows well-circumscribed hyperintense erosions (black arrows) in the humeral head,

with osteitis (white arrow) in the adjacent scapula. (b) T1-W FS gadolinium-enhanced image shows pannus enhances diffusely (Courtesy of J. Herman Kan)

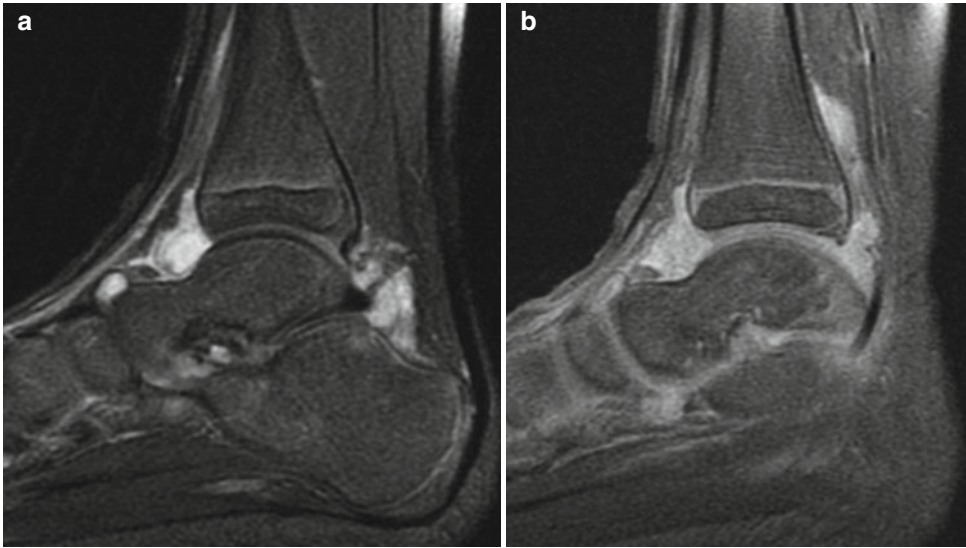


Fig. 20.20 Synovitis with enhancing pannus in a 6-year-old boy with JIA. (a) Sagittal T2-W image shows hyperintense thick material within the ankle joint. After administration of gadolinium (b, T1-W FS), all the hyper-

intense areas enhance, indicating they represent thickened synovium, not joint fluid. The cartilage appears intact (Courtesy of Tal Laor, Cincinnati Children's Hospital)

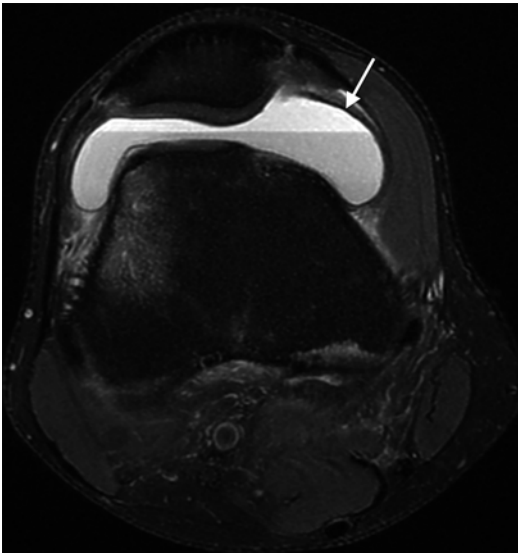


Fig. 20.21 Normal synovium. Axial PD FS image of a 17-year-old male after trauma shows normal hypointense non-thickened synovium (arrow). Note lipohemarthrosis and distal femoral marrow edema

lar synovium, which enhances, from inactive, fibrotic synovium, which does not [7, 13].

The rate of contrast enhancement and measurements of dynamic synovial enhancement may be

used to assess the degree of inflammatory response, but this is not routinely performed in clinical practice. Quantitative MRI assessment of synovial volumes also assesses response to therapy [17].

MRI is the most sensitive modality for detecting morphologic alterations in articular cartilage. T1-W FS 3-dimensional (3D) gradient echo (GRE) techniques reliably assess cartilage loss with relatively high sensitivity and specificity. Normal cartilage is hyperintense, and defects appear as hypointense foci. Subtle irregularities, cystic changes, and underlying desiccation are readily recognized. 3D data can be further analyzed, allowing quantitative assessment of cartilage volume. Thickness and contour may be mapped, with important implications in assessing therapeutic response and determining long-term prognosis (Fig. 20.25) [18]. As articular cartilage degenerates, microstructural alterations cause T2 relaxation time to increase. Indeed, in patients with JIA, the cartilage may demonstrate degeneration on T2 mapping, even when disease is apparently clinically quiescent or improving [5].

Additional GRE techniques for imaging pediatric hyaline and in particular articular cartilage

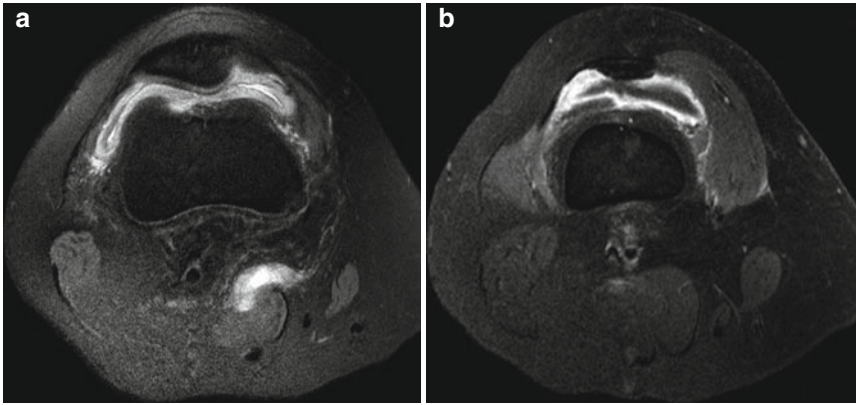


Fig. 20.22 Thickened synovium in a patient with JIA. (a) Axial PD FS image of the knee shows synovial thickening and hyperintensity along with a small amount of joint

fluid. (b) T1-W FS gadolinium-enhanced image shows diffuse enhancement of the thickened synovium, along with hypointense joint fluid

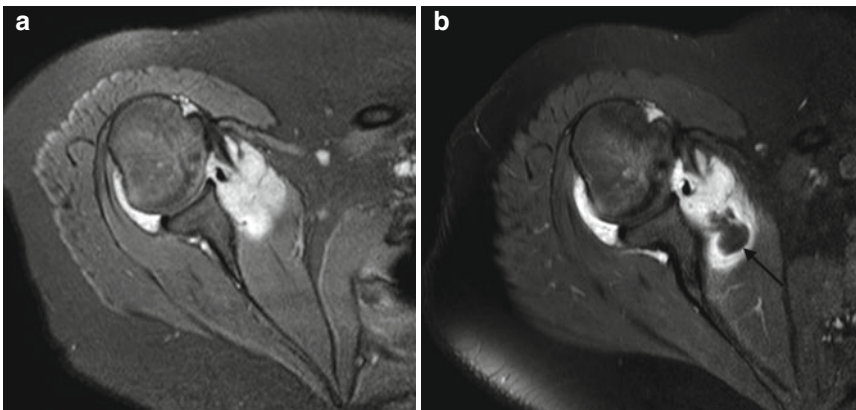


Fig. 20.23 Enhancing pannus in a 19-year-old girl with JIA. (a) T2-W FS axial image shows hyperintense fluid and pannus at the shoulder. (b) T1-W FS gadolinium-

enhanced axial image contrasts non-enhancing joint fluid (arrow) and enhancing pannus (Courtesy of J. Herman Kan)

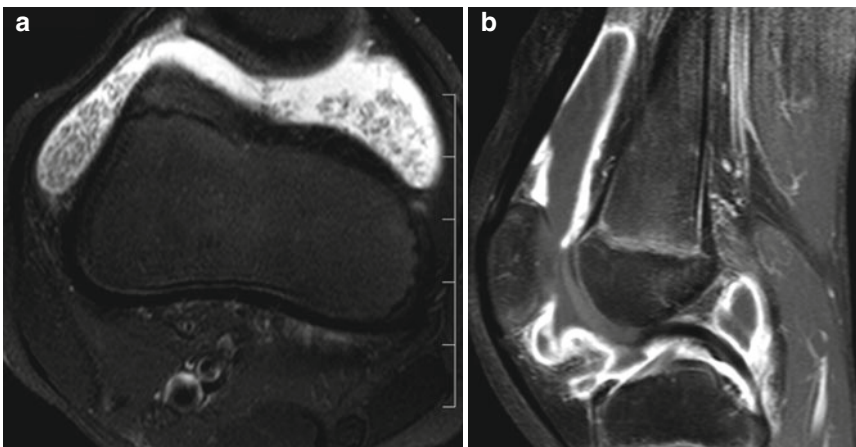


Fig. 20.24 Rice bodies in a 7-year-old girl. (a) Axial T2-W image demonstrates multiple intermediate-intensity rice bodies within hyperintense joint fluid. (b) Sagittal

T1-W FS gadolinium-enhanced image shows thick, enhancing synovium, but the rice bodies are occult

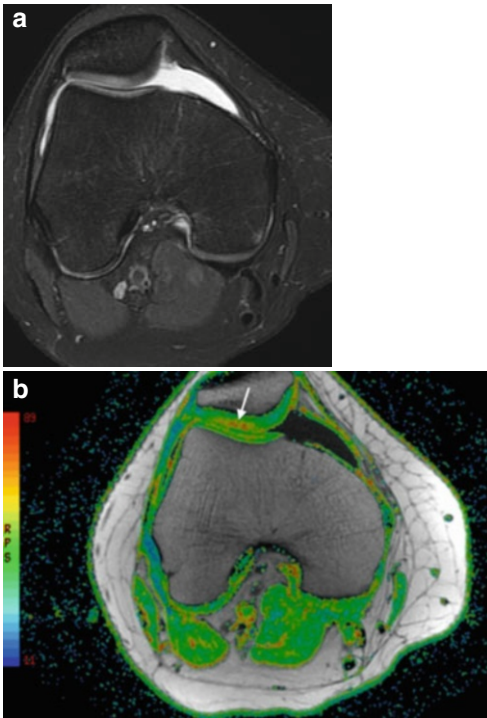


Fig. 20.25 T2 mapping of cartilage in a child with JIA. (a) Axial T2-W FS image shows that although the morphology is normal, there is relatively increased signal intensity in the articular cartilage of the lateral facet. (b) Corresponding T2 map at the same level. The hotter colors (oranges and reds) correspond to longer T2 relaxation times. There is replacement of the normal laminar configuration of the articular cartilage in the lateral facet by a focal area of abnormally increased T2 signal intensity (arrow). This likely reflects the effect of disease on cartilage microstructure, prior to morphologic change. The colors correspond to specific T2 relaxation times, which allows for quantitative, objective evaluation over time (Courtesy of Tal Laor, Cincinnati Children’s Hospital)

include such steady-state sequences as dual echo steady state (DESS), refocused steady-state free precession (SSFP), and water selective balanced steady-state free precession (WS-bSSFP). The DESS sequence, which combines two gradient echoes, provides high T2 contrast and depicts joint morphology well [19].

Osteitis, which may precede the development of bone erosions, appears hypointense on T1-W imaging and hyperintense on short tau inversion recovery (STIR) and T2-W imaging (see Fig. 20.19). Although often mistakenly described as “edema,” osteitis actually represents an inflam-

matory cellular infiltrate [20]. Erosions are also hypointense on T1-W and hyperintense on T2-W imaging, but their margins are well circumscribed, and there must be overlying cortical disruption. Enhancement within erosions indicates the presence of hypervascular pannus, implying active disease. Erosions and cartilage destruction are more common after skeletal maturity, when the cartilage has thinned [16].

Erosions are common at the wrist (see Fig. 20.18) and must be differentiated from normal carpal undulations. The latter, found in more than 50 % of children, are often seen in the capitate or hamate [21]. Erosion is more likely if there is edema, cartilage destruction, and synovial enhancement. In addition, erosions are more common at the bare areas of intra-articular bone (i.e., the nonarticular portions of metacarpal and metatarsal heads and bases), where there is no overlying cartilage [21].

MRI also assesses joint deformities and growth disturbances, especially in locations where radiography and ultrasound provide limited information, such as the sacroiliac joints and temporomandibular joints.

Regional Findings (Box 20.1)

Mandible. The mandible is subject to erosions, joint space narrowing, and growth disturbance.

Box 20.1: Imaging Features of Juvenile Idiopathic Arthritis (JIA) by Anatomic Region

Mandible	Short body and ramus Flat condyle, wide intercondylar joint Concave undersurface of the mandibular body (antegonial notching)
Cervical spine	Ankylosis of the upper cervical spine Affected vertebrae hypoplastic Erosion of the odontoid process
Hands/feet	Premature ossification Ankylosis of the tarsals and carpals Subluxation Periostitis of the metatarsals and metacarpals
Knee	Epiphyseal enlargement Wide intercondylar notch Squared lower pole of the patella

The temporomandibular joint (TMJ) is affected in up to 87 % of patients with JIA, especially in patients whose initial presentation was before age 4 [14]. Common findings include shortening of the body and ramus, flattening of the condyle, widening of the intercondylar joint, narrowing of the joint space, and abnormal concavity of the undersurface of the mandibular body (*antegonial notching*, Fig. 20.26) [7]. If there is active inflammation, contrast-enhanced MRI demonstrates typical findings of effusion, synovial enhancement, and marrow edema. Open and closed mouth dynamic assessment may depict abnormal joint motion, disk abnormalities, and growth disturbances.

Cervical Spine. The cervical spine is affected in about 60 % of patients [14], and patients with polyarticular or systemic JIA are most likely to have cervical spine involvement. Ankylosis may occur within 3–5 years of disease onset and is most common at the apophyseal joints at C2–3, though multiple levels are often affected (see Fig. 20.26). The associated vertebral bodies are often hypoplastic in transverse and anteroposterior dimensions, and disk spaces are narrow. Synovial proliferation may cause erosions of the odontoid process, and ligamentous insufficiency may lead to atlantoaxial instability. Atlantoaxial impaction may occur in young adults with polyarticular JIA.

Hands and Feet. Ankylosis of the carpal and tarsal bones may develop within 3–5 years of onset of disease [14] (see Fig. 20.8). Carpal bones of the wrist may ossify prematurely (uni- or bilaterally). Subluxation, dislocation, and flexion/extension deformities are more common in the hands and feet than elsewhere (see Fig. 20.12); if the wrist is affected, it deviates in a radial direction. Periostitis may lead to a squared off appearance of the metacarpals and metatarsals (see Fig. 20.4).

Knee. Overall, the knee is the most commonly affected joint. Standing radiographs best assess for joint space narrowing and other complications. The knee may develop the classic appearance of epiphyseal enlargement, widened intercondylar notch, and squared lower pole of the patella (see Figs. 20.6 and 20.7). These findings are also sometimes seen with hemophilia.



Fig. 20.26 Cervical spine deformity and fusion in a 10-year-old girl with systemic polyarticular JIA. The laminae are fused from C2 through C6, and the vertebral bodies are unusually tall and narrow. Intervertebral disks are narrowed, with fusion across C2–3. Antegonial notching (*arrow*) at the mandible

1.1 Enthesitis-Related Arthritis (ERA)

Several arthritides share the common feature of enthesopathy (inflammation of ligaments or tendons where they attach to bone). These include juvenile onset ankylosing spondylitis, reactive arthritis, and undifferentiated spondyloarthritis. Diagnosis requires at least two of the following criteria: onset in a male age 8 or older, HLA-B27 positivity (or positive family history), spinal or sacroiliac pain, and anterior uveitis. The discussion below is predominantly limited to juvenile onset ankylosing spondylitis.

Ankylosing spondylitis usually manifests during adulthood. When encountered in children, it

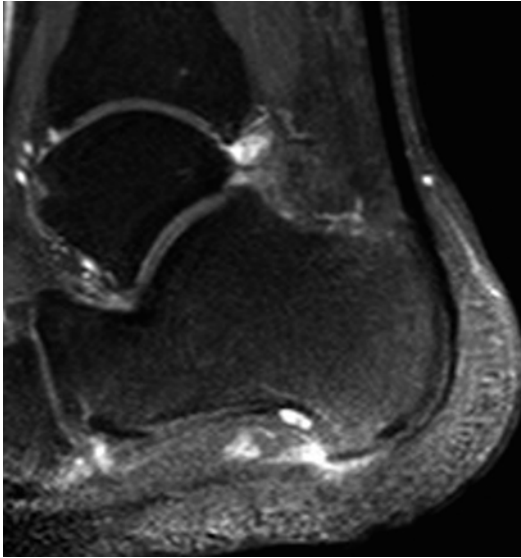


Fig. 20.27 Calcaneal spur in an 8-year-old boy with ERA. Sagittal T1-W FS gadolinium-enhanced image shows spur with enhancement at the insertion of the plantar aponeurosis (Courtesy of J. Herman Kan)

is commonly seen in male patients in late adolescence. Unlike in adults, it typically presents with early extra-axial involvement and a higher frequency of peripheral arthritis and enthesitis. The hips, knees, and shoulders are most frequently involved. Although a cause of long-term disability, sacroiliitis is often initially asymptomatic, and fewer than 25 % of children complain of spine or sacroiliac signs or symptoms [22].

Imaging (Box 20.2)

Radiographic findings include joint space narrowing and erosions, which, unlike in the adult population, do not typically evolve into severe

Box 20.2: Enthesitis-Related Arthritis (ERA)

Common	Enthesitis at calcaneus (at the Achilles tendon or plantar aponeurosis) Hips, knees, shoulders Joint space narrowing, erosions
<25 %	Spine or sacroiliac joints Radiographs positive after 5–10 years: bilateral, symmetric MRI positive sooner: T2 hyperintensity and enhancement

joint destruction. Enthesitis, a common element, may present as a bony erosion, lucency, or spur. Spurs are especially common at the calcaneus, either at the insertion of the Achilles tendon or at the insertion of the plantar aponeurosis (Fig. 20.27). Not uncommonly, periostitis may be present along short tubular bones of the hand and, in some cases, along other bones.

However, radiographic abnormalities in the axial skeleton take much longer to appear than those in the peripheral skeleton. Radiographic evidence of sacroiliac arthritis is almost always seen well before any radiographic abnormality becomes apparent in the spine. Even this is seen only after clinical symptoms have progressed to an advanced stage, after disease has been present for 5–10 years. Bilateral asymmetrical involvement of the sacroiliac joints is the most common pattern (Fig. 20.28). Occasionally unilateral involvement mimics tuberculosis and subacute septic arthritis. Unlike in JIA, the cervical spine is usually normal. Syndesmophyte formation is rarely seen in children, and the “bamboo spine” typical of adults is generally not encountered in children. Sacroiliac arthritis is almost always seen well before any radiographic abnormality of the spine.

MRI evaluation of the sacroiliac joints allows earlier identification of sacroiliitis, making this a useful screening tool in patients with suspected ERA who have no spine or sacroiliac symptoms. Dynamic contrast-enhanced MRI is useful for



Fig. 20.28 Sacroiliitis in a 15-year-old girl with ERA. Asymmetrical (left worse than right) irregularity of the sacroiliac joints and iliac osteitis on the left

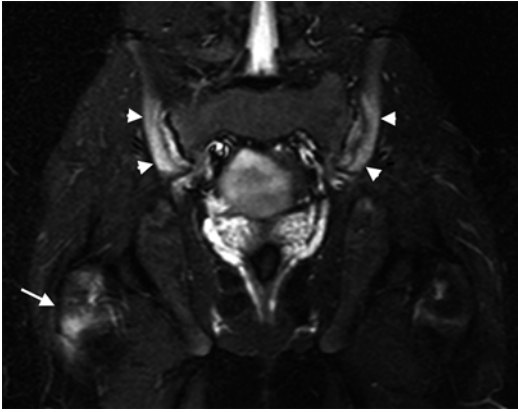


Fig. 20.29 Osteitis in a 16-year-old boy with ERA. Coronal T2-W image shows marrow hyperintensity consistent with enthesitis in the right greater trochanter (*arrow*). In addition, there is bilateral sacroiliitis, with hyperintense signal within the joints and juxtasyovial iliac bone osteitis (*arrowheads*) (Courtesy of J. Herman Kan)

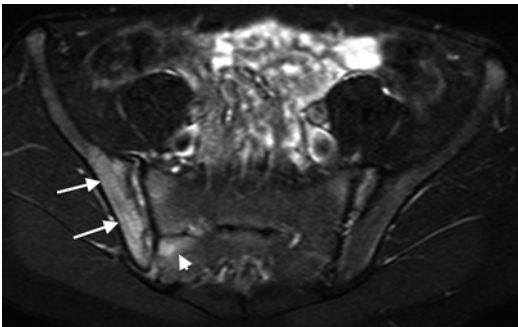


Fig. 20.30 Sacroiliitis in a 13-year-old boy with ERA. Axial T2-W image shows hyperintensity at the right and to a lesser extent left sacroiliac joints. In addition, there is right iliac osteitis present (*arrows*), as well as right greater than left sacral alar osteitis (*arrowhead*) (Courtesy of J. Herman Kan)

diagnosing both acute and chronic abnormalities in the sacroiliac joints [23, 24]. Typical findings include subarticular marrow edema or osteitis and T2 hyperintensity at the sacroiliac joints (Figs. 20.29 and 20.30). With more advanced disease, erosions on T1-W sequences and synovial enhancement may be evident.

US and MRI are both useful for assessing the small joints of the hands and feet. US demonstrates thickening of the tendons as well as peritendinous fluid. Typical MRI findings of enthesitis include swelling and T2 hyperinten-

sity at the tendons and ligaments where they attach to bone. There may also be T2 hyperintensity within the adjacent bone, and bursae may be distended and soft tissues edematous [24]. MRI may delineate tenosynovitis and enthesitis (Fig. 20.31), along with subclinical ligament rupture.

2 Hemophilic Arthropathy

This X-linked autosomal recessive disorder affects 1 in 10,000 boys and typically presents before age 20. There are two subtypes, both due to an abnormal coagulation factor. Deficiency in clotting factor VIII leads to subtype A, and deficiency in plasma factor IX results in subtype B. Clinical presentation and imaging findings are similar for both forms of the disease. Patients have a propensity to bleed after minor trauma, especially into the joints. Indeed, 90 % of patients with severe hemophilia eventually develop joint disease [25]. The initial hemorrhagic episode often occurs before age 10.

The most commonly affected joints are the knee, ankle, and elbow. Bleeding usually begins in the synovium and extends to involve the joint space itself. Chondrocytes and macrophages absorb released iron, and hydrolytic enzymes then incite an inflammatory response. Inflamed synovium is prone to rebleed, and a vicious cycle of recurrent bleeding ensues. Epiphyseal overgrowth occurs as part of the inflammatory response.

Bleeding into the bone and soft tissues may lead to development of pseudotumors in up to 2 % of patients, generally in those with severe coagulopathy [26]. The resultant chronic, painless, encapsulated, slowly expanding mass may result from minor trauma and is usually an incidental finding. Bleeding into the subperiosteum occurs uncommonly.

Treatment of hemophilia generally involves replacing missing clotting factors, preferably prior to onset of joint damage. However, up to 30 % of patients produce antibodies to these clotting factors, leading to increased risk of uncontrolled bleeding [27]. Affected joints may be treated with radionuclide or open synovectomy [25].

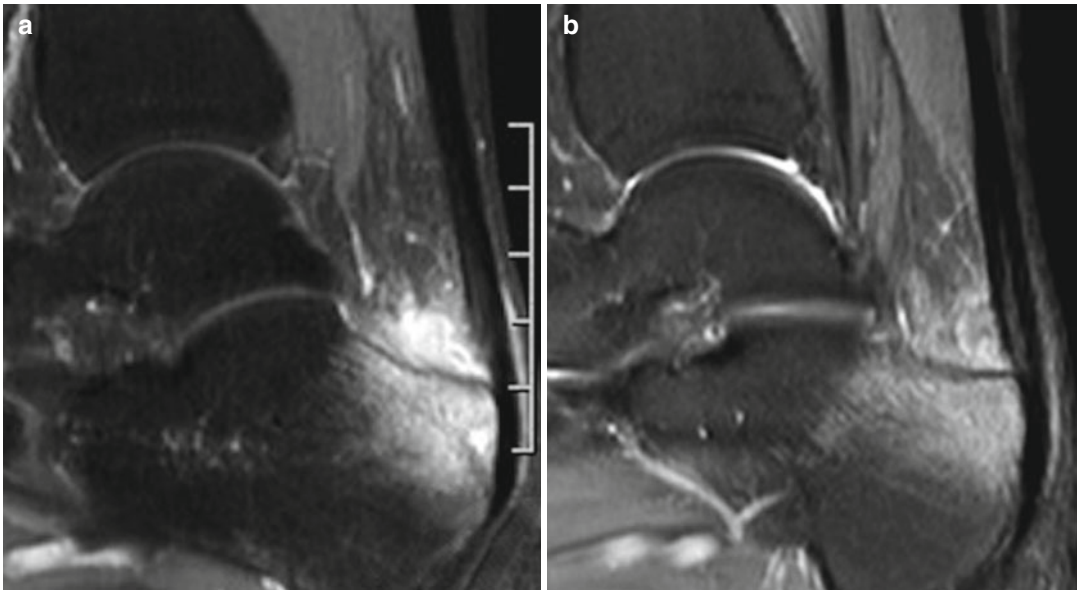


Fig. 20.31 Enthesitis in a 17-year-old girl with ERA. (a) Sagittal T1-W FS gadolinium-enhanced image shows enhancement in the calcaneal body and tuberosity at the Achilles insertion, as well as in Kager fat pad. (b) Sagittal

PD FS image shows corresponding hyperintensity, as well as increased intrasubstance signal within the distal Achilles tendon (Courtesy of J. Herman Kan)

Imaging (Box 20.3)

Radiographs. Joint effusion and hemarthrosis are early findings (Fig. 20.32). Synovial hypertrophy and hemosiderin deposition appear as nonspecific soft tissue swelling. However, with progressive articular and periarticular pathology, osseous erosions and subchondral cysts become evident (Fig. 20.33). Joint space narrowing due to cartilage thinning may eventually become evident on radiographs. Inflammation and hyperemia may lead to epiphyseal overgrowth and osteopenia, with early growth plate closure. At the knee, epiphyseal overgrowth is common, with widening of the intercondylar notch, flattened contours of the condyles, squaring of the patella, and cartilage as well as subchondral bony destruction (Fig. 20.34).

The Arnold-Hilgartner system grades osteochondral and soft tissue radiographic findings on a scale of 0–5 and can predict the presence of synovial hypertrophy (Table 20.2). This system is commonly employed in the USA [28, 29]. The Pettersson scoring system provides a framework for analysis of radiographic findings, wherein a cumulative score is assigned based on the pres-

Box 20.3: Imaging Features of Hemophilic Arthropathy

Hemarthrosis: knee, ankle, elbow

Radiographic stages described by Arnold-Hilgartner system (Table 20.2)

US Evaluates synovial vascularity, hemarthrosis

MRI

Early Joint effusion with fluid-fluid level

Synovial hypertrophy

Focal cartilage erosion

Synovial hemosiderin deposition

Synovial T2 hyperintensity (inflammation)

Chronic Hypointense fibrotic synovium

Synovial hemosiderin deposition

Cartilage thinning, bone erosion

Subchondral cysts

ence or absence of multiple findings. This scoring system has been adopted by the World Federation of Hemophilia [30].



Fig. 20.32 Joint effusion in a young boy with hemophilia. Bones are normal (Courtesy of J. Herman Kan)



Fig. 20.33 Elbow joint space narrowing and osseous erosions at the trochlea, proximal ulna, and radial head in a 15-year-old boy with hemophilia

Pseudotumors are encountered most often in the soft tissues but also occur in the bone or subperiosteum. The femur, pelvis, tibia, and hand are the most common locations of osseous pseudotumors (in descending order of frequency)

[26]. A soft tissue pseudotumor appears as a hemorrhagic soft tissue mass, sometimes eroding adjacent bone.

Bony pseudotumors appear as well-defined, expansile, lytic uni- or multilocular eccentric or intramedullary masses (Fig. 20.35). There may be cortical thinning and erosions, endosteal scalloping, peripheral sclerosis, and pathological fractures. Dystrophic calcification may be seen, along with subperiosteal new bone formation and aggressive periosteal reaction. Pseudotumors may completely replace affected bone. The differential is broad, including many lucent bone lesions. Peripheral curvilinear calcific struts extending into the soft tissues are characteristic.

US. Doppler US may be employed to evaluate synovial vascularity and to evaluate for hemarthroses (Fig. 20.36) [31]. US may also be used to follow soft tissue tumors.

CT. Computed tomography (CT) may demonstrate trabeculae crossing the radiolucent pseudotumor as well as characteristic calcific struts.

MRI. MRI allows more precise evaluation of joint involvement in early as well as advanced disease. Scoring systems (such as the semiquantitative Denver scale) facilitate assessment of treatment response [27]. Early MRI finding in joints affected by hemophilia include effusions with fluid-fluid levels, synovial hypertrophy, and focal areas of cartilage erosion. Synovial hemosiderin deposition is often apparent, with susceptibility artifact appearing dark on GRE sequences. Hemosiderin also appears markedly hypointense on T1- and T2-W sequences (Fig. 20.37). Cartilage destruction is best recognized on FS proton density (PD) or DESS sequences (Fig. 20.38) [31]. Synovial hypertrophy may be identified as hyperintense thickening on T2-W FS and on T1-W gadolinium-enhanced sequences (Fig. 20.39). In the chronic phase of disease, fibrotic synovium appears hypointense, and there may be cartilage thinning, bony erosions, and subchondral cysts (Fig. 20.40).

A pseudotumor appears as a hemorrhagic intraosseous and/or soft tissue mass with a rim that is hypointense on both T1- and T2-W imaging (Fig. 20.41). Enhancement is typically thin and nodular. Intralesional methemoglobin and

Fig. 20.34 Knee deformity in a boy with hemophilia. (a, b) The intercondylar notch is enlarged, the femoral condyles are overgrown, and there is joint space narrowing with bony erosions. Large, dense joint effusion (Courtesy of J. Herman Kan)

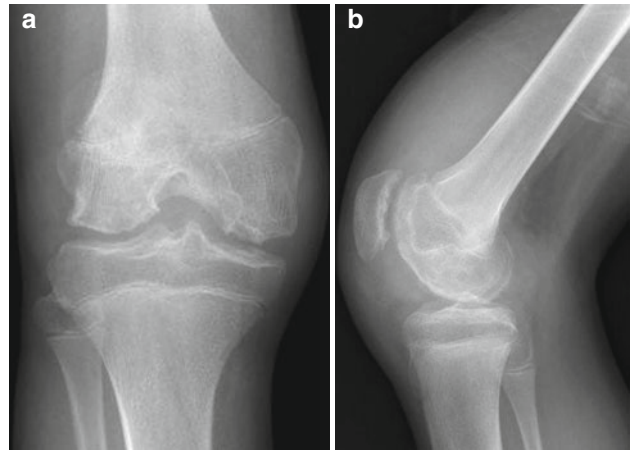


Table 20.2 Arnold-Hilgartner staging for hemophilia

Stage	Findings in joint
0	Normal
1	Soft tissue swelling; normal bones
2	Epiphyseal osteoporosis and overgrowth No erosions or joint space narrowing
3	Early subchondral bone cysts Knee and humerus: wide intercondylar notch Squared patella Joint space intact
4	Narrowed joint space Other findings of stage 3 more advanced
5	Narrowed joint space Fibrous joint contracture Marked epiphyseal enlargement Disorganization of joint

Adapted from Arnold and Hilgartner [28]



Fig. 20.35 Pathological fractures through pseudotumors in the first and fifth digits in a teen with hemophilia

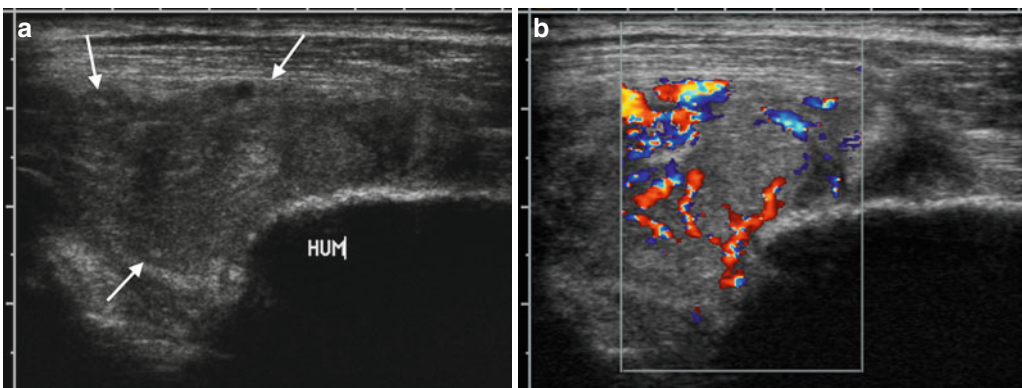


Fig. 20.36 Synovial proliferation in the elbow of a 14-year-old boy with factor VIII deficiency. (a) US demonstrates a heterogeneous mass (arrows) in the elbow

joint with (b) increased vascularity. “Hum” denotes “humerus” (Same patient as Fig. 20.39)



Fig. 20.37 Hemosiderin deposition in the ankle joint of a 16-year-old boy with hemophilia, without erosions. Arrows indicate hypointense hemosiderin

hemosiderin are evident, and there may be fluid-fluid levels.

3 Pigmented Villonodular Synovitis

Another relatively uncommon condition in children, pigmented villonodular synovitis (PVNS) is a benign, hypertrophic process that affects the synovium, bursas, and tendon sheaths. It usually presents in the third or fourth decade of life but has been reported in patients as young as 4 years of age [32]. Pediatric PVNS may be associated with vascular lesions, cherubism, lymphedema, Noonan and multiple lentigines syndrome, and jaw lesions [33]. In adults, lesions are usually solitary, but children are more likely to have polyarticular or multifocal involvement [33].

At any given location, either diffuse or localized disease may develop. The diffuse form typically affects the large joints, especially the knee (66–80 %) [33]. Other joints that may be affected include the hip, ankle, shoulder, and elbow, in decreasing order of frequency. The focal nodular form is more common in the distal extremities, typically the fingers. A similar process may also affect extra-articular spaces,

such as tendon sheaths (PVNTS, or pigmented villonodular tenosynovitis) and bursas (PVNB, or pigmented villonodular bursitis). PVNTS, also termed giant cell tumor of the tendon sheath, is especially common in the hand and wrist. Patients with extra-articular PVNTS or PVNB present with a soft tissue mass and pain, whereas those with intra-articular PVNS usually complain of pain, joint swelling, and occasionally dysfunction.

Proliferation may be villous, nodular, or villonodular. The affected tissue in the diffuse intra-articular form of PVNS appears tan or yellow because of hemosiderin/fat deposition in the proliferative synovium. Epithelioid and giant cells are arrayed within a fibrous stroma that contains hemosiderin and lipid [34]. While the diffuse form is more infiltrative and demonstrates more prominent deposits of hemosiderin, the localized form tends to be well defined, with a collagenous pseudocapsule. Etiology is uncertain, but cytogenetic aberrations are evident in most cases of PVNS, suggesting a neoplastic origin [33].

Surgical resection is the mainstay of treatment for PVNS. If resection is incomplete, radiation or chemotherapy may be employed. However, incidence of local recurrence is as high as 50 % [2].

In the vast majority of cases, PVNS is limited to benign proliferation of the synovium (or bursas and tendon sheaths). However, a malignant form has been described in patients as young as 12 years old. Malignant PVNS is characterized by development of a sarcomatous tumor that histologically resembles PVNS within a joint that currently is or previously was affected by PVNS. The knee is most often involved [35].

Imaging (Box 20.4)

The classic early radiographic finding of PVNS is soft tissue swelling without calcification. Joint space is initially preserved. Extrinsic erosions with well-defined sclerotic borders develop on both sides of the joint, especially in joints where ligaments limit expansion or where joint capacity is small, such as the hip, shoulder, elbow, and ankle (Fig. 20.42). Erosive changes are less common at the more capacious knee (Fig. 20.43) [36]. As disease progresses and the cartilage

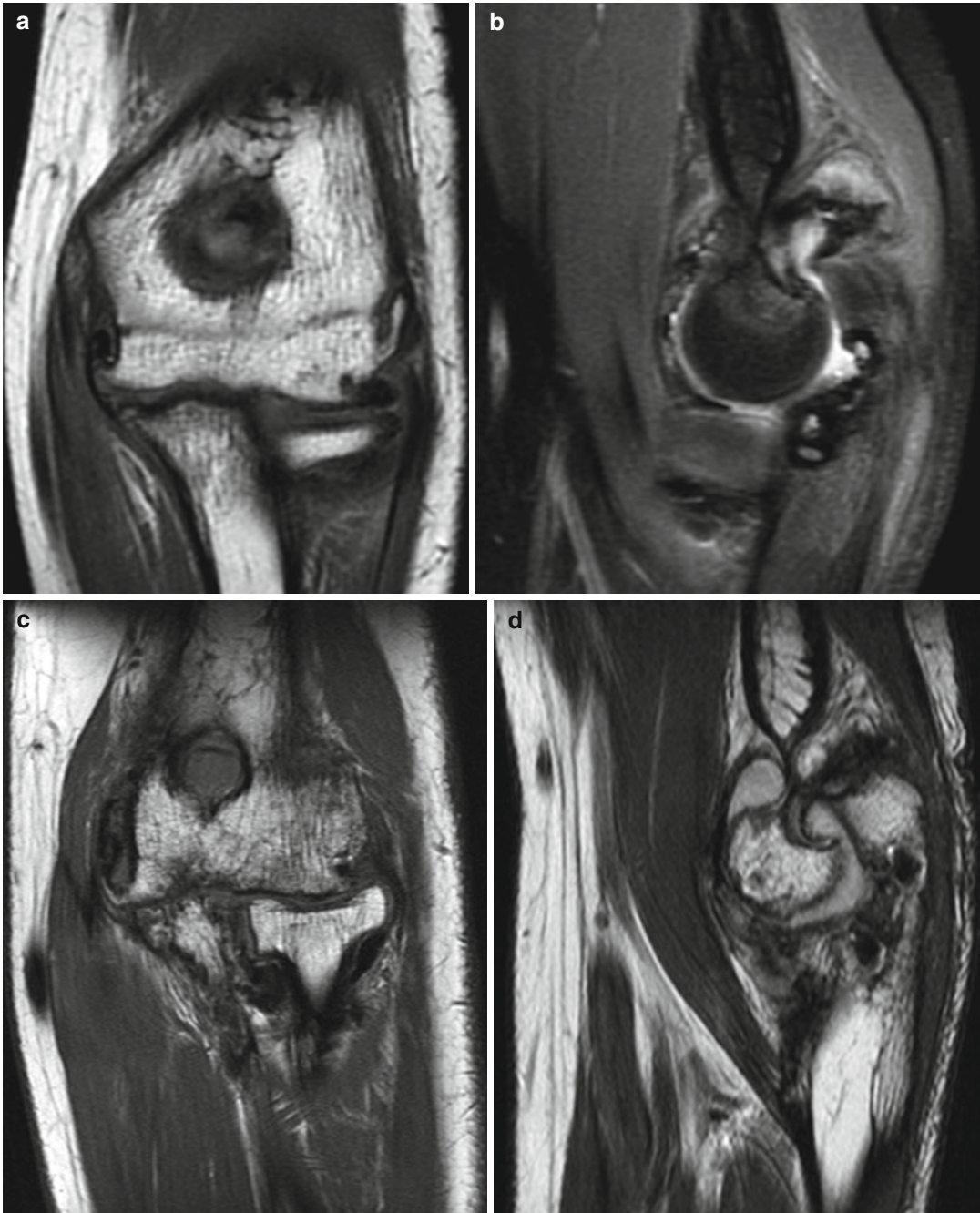


Fig. 20.38 Progressive arthropathy in a 12-year-old (a, b) and then 19-year-old (c, d) male with factor VIII deficiency. (a) Coronal T1-W image shows joint space narrowing and small subchondral cysts. (b) Sagittal PD FS image shows intra-articular joint fluid as well as fluid within the subchondral cysts and hemosiderin deposition

along mildly thickened synovium. (c) Seven years later, coronal T1-W image shows high-grade chondral thinning with cortical irregularity, progressive joint space narrowing, periarticular marrow edema, and hemosiderin deposition. (d) Sagittal PD image shows susceptibility artifact from hemosiderin deposition within subchondral cysts

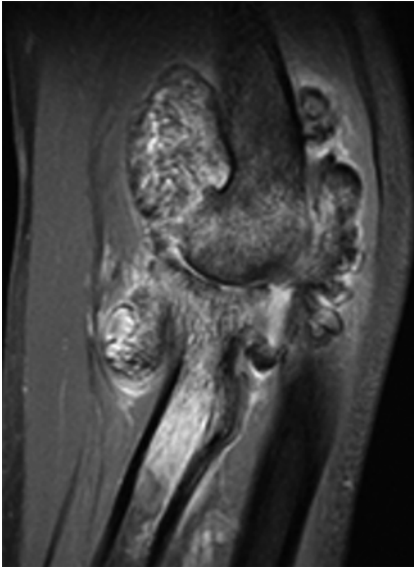


Fig. 20.39 Mass-like synovial proliferation in a 14-year-old boy with factor VIII deficiency. T1-W FS gadolinium-enhanced sagittal image demonstrates heaped up masses of synovium that demonstrate heterogeneous enhancement with peripheral hypointensity indicating hemosiderin deposition. There is joint space narrowing and marrow edema, as well as small cortical erosions (Same patient as Fig. 20.36)

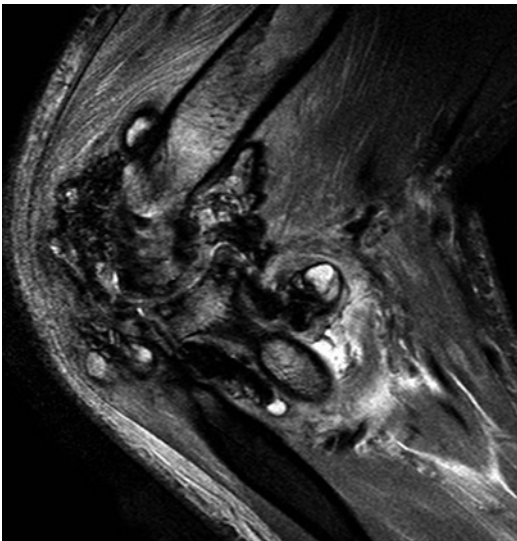


Fig. 20.40 Hemophilic arthritis in an 11-year-old boy. Sagittal T2-W FS image of the elbow demonstrates extensive susceptibility artifact related to hypertrophied and hemosiderin-laden synovium. There is subcutaneous and muscular edema, along with distal humeral and proximal radial marrow edema. (Courtesy of J. Herman Kan)

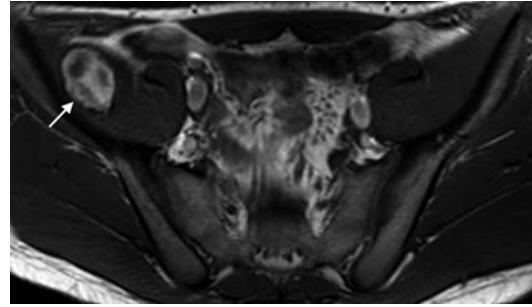


Fig. 20.41 Soft tissue pseudotumor in a patient with hemophilia. Axial T1-W image shows a large pseudotumor (arrow) within the right iliacus muscle. Note heterogeneous areas of T1 shortening within the pseudotumor, consistent with hemosiderin (Courtesy of J. Herman Kan)

Box 20.4: Imaging Features of Pigmented Villonodular Synovitis (PVNS)

Radiography

Early	Soft tissue swelling Preservation of joint space
Mid	Extrinsic erosions with sclerotic borders In tight joints (hip, shoulder, elbow, ankle) Less common in the knee
Late	Cartilage erosion → joint space narrowing Loose bodies, geodes, osteophytes

Early findings on MRI

Focal or nodular synovial thickening
Hemosiderin deposition more with diffuse than localized form
Intermediate or low signal on all sequences
T2: linear hypointensity along periphery of the synovium

becomes eroded, joint space narrowing may develop, along with osteopenia, loose bodies, geodes, and osteophytes. These findings also are more common in relatively tight joints. US demonstrates vascular, hypochoic, mass-like synovial proliferation (Fig. 20.44).

MRI demonstrates diffuse or focal nodular synovial thickening, depending on whether the patient has the diffuse or localized form of disease (Fig. 20.45). Synovium has low or intermediate signal on all pulse sequences; T2-W sequences reveal linear hypointense signal along

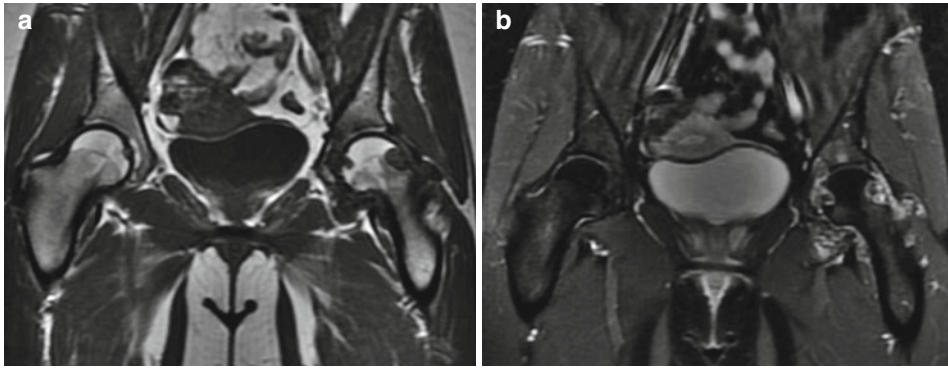


Fig. 20.42 Erosions in a 21-year-old female with PVNS. (a) Coronal T1-W image shows well-circumscribed erosions in the left femoral head. (b) Coronal T1-W FS gadolinium-enhanced image shows synovial enhancement extending into the erosions (Courtesy of J. Herman Kan)



Fig. 20.43 Nodular PVNS in a 14-year-old girl. Sagittal T1-W (a), T1-W FS gadolinium-enhanced (b), and IR (c) images show that despite the presence of a large, heterogeneous mass encasing the posterior cruciate ligament, there are no significant osseous erosions. Peripheral hypointense hemosiderin deposition

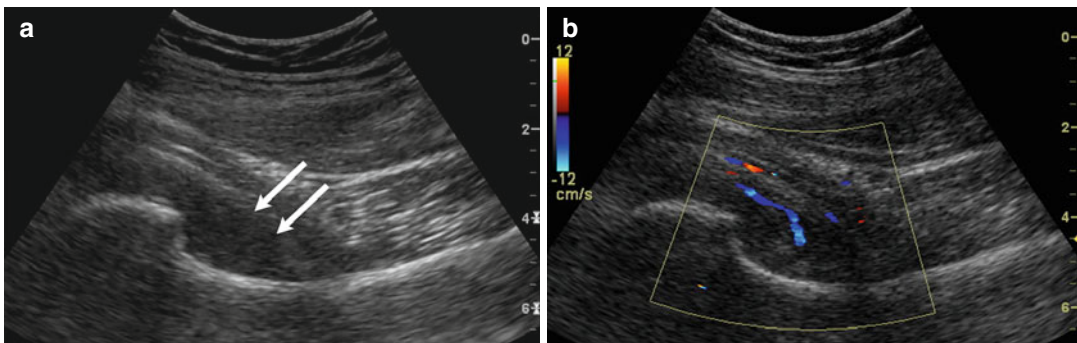


Fig. 20.44 PVNS in a 17-year-old girl. Longitudinal hip US (a) shows synovial thickening with fine internal solid echogenicity (arrows). There is internal vascularity on color Doppler (b) (Reprinted from Doria and Babyn [38], copyright Elsevier 2013) (Image courtesy of Andrea Doria)

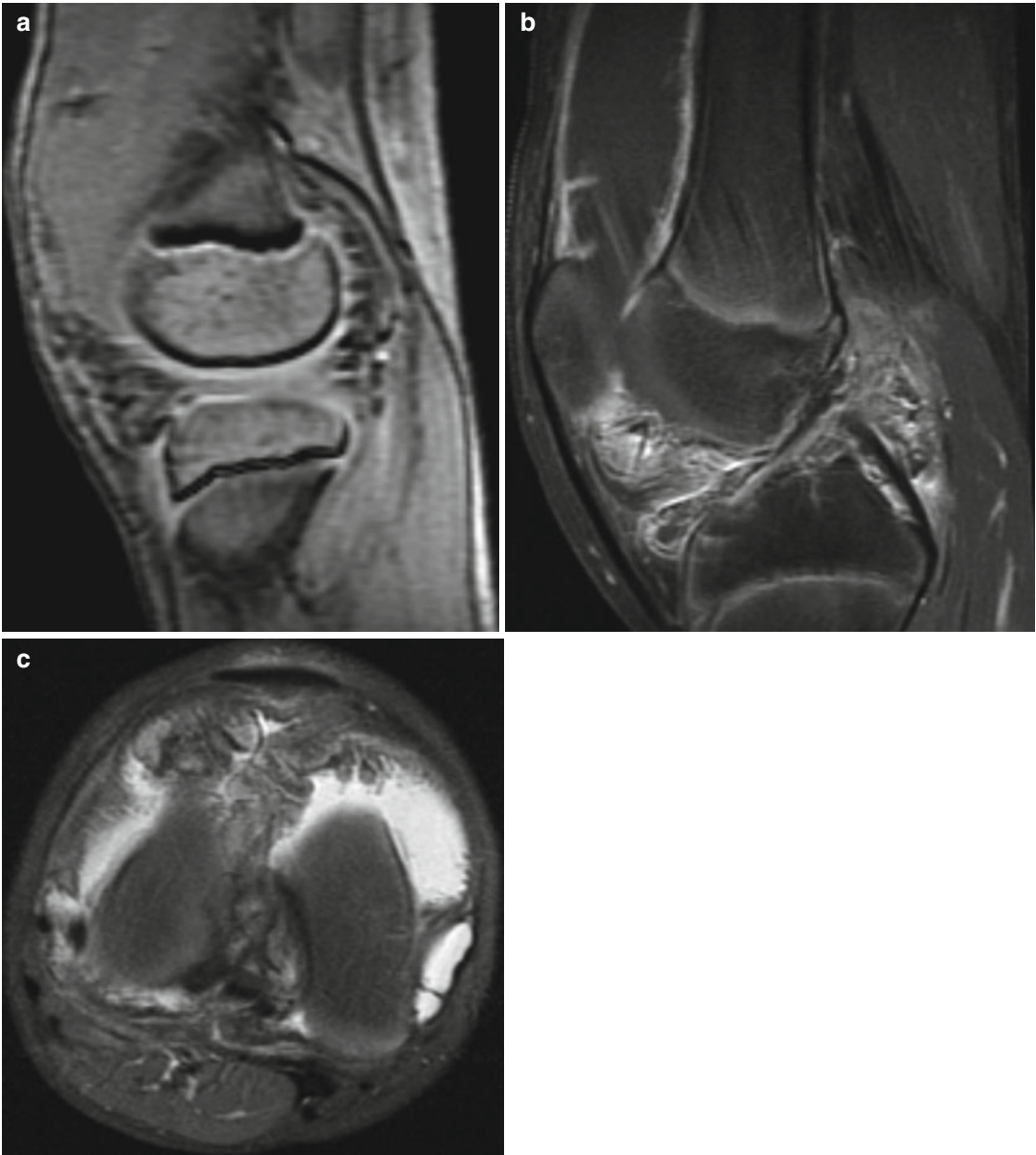


Fig. 20.45 Diffuse PVNS. (a) Sagittal GRE scout image demonstrates blooming artifact in the anterior and posterior knee joint. (b) Sagittal T1-W FS gadolinium-enhanced image shows corresponding diffuse serpiginous enhance-

ment, with mild thickening of suprapatellar synovium. Large suprapatellar joint effusion. (c) Axial PD FS image shows diffuse nodularity with foci of hypointense hemosiderin (Courtesy of Tal Laor, Cincinnati Children's Hospital)

the periphery of thickened synovium, secondary to hemosiderin deposition. Hemosiderin deposition is more pronounced with the diffuse than with the localized form. “Blooming” of susceptibility artifact is apparent with GRE imaging. Enhancement is usually robust and homogeneous. A joint effusion is common in large joints.

Differential Diagnosis. Both hemophilia and hemangioma may also result in hemosiderin deposition within a joint as a result of repetitive intra-articular hemorrhage. However, the clinical history of hemophilia allows differentiation, as does the typical vascular appearance of hemangioma.

References

- Jordan A, McDonagh JE. Juvenile idiopathic arthritis: the paediatric perspective. *Pediatr Radiol.* 2006;36(8):734–42.
- Kim HK, Zbojniewicz AM, Merrow AC, Cheon JE, Kim IO, Emery KH. MR findings of synovial disease in children and young adults: part 1. *Pediatr Radiol.* 2011;41(4):495–511; quiz 545–496.
- Petty RE, Southwood TR, Manners P, Baum J, Glass DN, Goldenberg J, He X, Maldonado-Cocco J, Orozco-Alcala J, Prieur AM, Suarez-Almazor ME, Woo P, R. International League of Associations. International League of Associations for Rheumatology classification of juvenile idiopathic arthritis: second revision, Edmonton, 2001. *J Rheumatol.* 2004;31(2):390–2.
- Wallace CA, Levinson JE. Juvenile rheumatoid arthritis: outcome and treatment for the 1990s. *Rheum Dis Clin North Am.* 1991;17(4):891–905.
- Kim HK, Laor T, Graham TB, Anton CG, Salisbury SR, Racadio JM, Dardzinski BJ. T2 relaxation time changes in distal femoral articular cartilage in children with juvenile idiopathic arthritis: a 3-year longitudinal study. *AJR Am J Roentgenol.* 2010;195(4):1021–5.
- Petersson H, Rydholm U. Radiologic classification of knee joint destruction in juvenile chronic arthritis. *Pediatr Radiol.* 1984;14(6):419–21.
- Johnson K. Imaging of juvenile idiopathic arthritis. *Pediatr Radiol.* 2006;36(8):743–58.
- Reed MH, Wilmot DM. The radiology of juvenile rheumatoid arthritis. A review of the English language literature. *J Rheumatol Suppl.* 1991;31:2–22.
- Lang BA, Schneider R, Reilly BJ, Silverman ED, Laxer RM. Radiologic features of systemic onset juvenile rheumatoid arthritis. *J Rheumatol.* 1995;22(1):168–73.
- Sureda D, Quiroga S, Arnal C, Boronat M, Andreu J, Casas L. Juvenile rheumatoid arthritis of the knee: evaluation with US. *Radiology.* 1994;190(2):403–6.
- Haslam KE, McCann LJ, Wyatt S, Wakefield RJ. The detection of subclinical synovitis by ultrasound in oligoarticular juvenile idiopathic arthritis: a pilot study. *Rheumatology (Oxford).* 2010;49(1):123–7.
- Wakefield RJ, Gibbon WW, Conaghan PG, O'Connor P, McGonagle D, Pease C, Green MJ, Veale DJ, Isaacs JD, Emery P. The value of sonography in the detection of bone erosions in patients with rheumatoid arthritis: a comparison with conventional radiography. *Arthritis Rheum.* 2000;43(12):2762–70.
- Lamer S, Sebag GH. MRI and ultrasound in children with juvenile chronic arthritis. *Eur J Radiol.* 2000;33(2):85–93.
- Sheybani EF, Khanna G, White AJ, Demertzis JL. Imaging of juvenile idiopathic arthritis: a multimodality approach. *Radiographics.* 2013;33(5):1253–73.
- Damasio MB, Malattia C, Martini A, Toma P. Synovial and inflammatory diseases in childhood: role of new imaging modalities in the assessment of patients with juvenile idiopathic arthritis. *Pediatr Radiol.* 2010;40(6):985–98.
- Gyllys-Morin VM, Graham TB, Blebea JS, Dardzinski BJ, Laor T, Johnson ND, Oestreich AE, Passo MH. Knee in early juvenile rheumatoid arthritis: MR imaging findings. *Radiology.* 2001;220(3):696–706.
- Workie DW, Graham TB, Laor T, Rajagopal A, O'Brien KJ, Bommer WA, Racadio JM, Shire NJ, Dardzinski BJ. Quantitative MR characterization of disease activity in the knee in children with juvenile idiopathic arthritis: a longitudinal pilot study. *Pediatr Radiol.* 2007;37(6):535–43.
- Kight AC, Dardzinski BJ, Laor T, Graham TB. Magnetic resonance imaging evaluation of the effects of juvenile rheumatoid arthritis on distal femoral weight-bearing cartilage. *Arthritis Rheum.* 2004;50(3):901–5.
- Mosher TJ, Dardzinski BJ. Cartilage MRI T2 relaxation time mapping: overview and applications. *Semin Musculoskelet Radiol.* 2004;8(4):355–68.
- Ostergaard M, Peterfy C, Conaghan P, McQueen F, Bird P, Ejlertsen B, Shnier R, O'Connor P, Klarlund M, Emery P, Genant H, Lasserre M, Edmonds J. OMERACT Rheumatoid Arthritis Magnetic Resonance Imaging Studies. Core set of MRI acquisitions, joint pathology definitions, and the OMERACT RA-MRI scoring system. *J Rheumatol.* 2003;30(6):1385–6.
- Kan JH. Juvenile idiopathic arthritis and enthesitis-related arthropathies. *Pediatr Radiol.* 2013;43 Suppl 1:S172–80.
- Rosenberg AM. Juvenile onset spondyloarthropathies. *Curr Opin Rheumatol.* 2000;12(5):425–9.
- Bollow M, Biedermann T, Kannenberg J, Paris S, Schauer-Petrowski C, Minden K, Schontube M, Hamm B, Sieper J, Braun J. Use of dynamic magnetic resonance imaging to detect sacroiliitis in HLA-B27 positive and negative children with juvenile arthritides. *J Rheumatol.* 1998;25(3):556–64.
- Daldrup-Link HE, Steinbach L. MR imaging of pediatric arthritis. *Magn Reson Imaging Clin N Am.* 2009;17(3):451–67, vi.
- Hilgartner MW. Current treatment of hemophilic arthropathy. *Curr Opin Pediatr.* 2002;14(1):46–9.
- Park JS, Ryu KN. Hemophilic pseudotumor involving the musculoskeletal system: spectrum of radiologic findings. *AJR Am J Roentgenol.* 2004;183(1):55–61.
- Maclachlan J, Gough-Palmer A, Hargunani R, Farrant J, Holloway B. Haemophilia imaging: a review. *Skeletal Radiol.* 2009;38(10):949–57.
- Arnold WD, Hilgartner MW. Hemophilic arthropathy. Current concepts of pathogenesis and management. *J Bone Joint Surg Am.* 1977;59(3):287–305.
- Ng WH, Chu WC, Shing MK, Lam WW, Chik KW, Li CK, Li CK, Ling SC. Role of imaging in management of hemophilic patients. *AJR Am J Roentgenol.* 2005;184(5):1619–23.
- Kilcoyne RF, Nuss R. Radiological assessment of haemophilic arthropathy with emphasis on MRI findings. *Haemophilia.* 2003;9 Suppl 1:57–63; discussion 63–54.

31. Doria AS. State-of-the-art imaging techniques for the evaluation of haemophilic arthropathy: present and future. *Haemophilia*. 2010;16 Suppl 5:107–14.
32. Neubauer P, Weber AK, Miller NH, McCarthy EF. Pigmented villonodular synovitis in children: a report of six cases and review of the literature. *Iowa Orthop J*. 2007;27:90–4.
33. Murphey MD, Rhee JH, Lewis RB, Fanburg-Smith JC, Flemming DJ, Walker EA. Pigmented villonodular synovitis: radiologic-pathologic correlation. *Radiographics*. 2008;28(5):1493–518.
34. Goldman AB, DiCarlo EF. Pigmented villonodular synovitis. Diagnosis and differential diagnosis. *Radiol Clin North Am*. 1988;26(6):1327–47.
35. Bertoni F, Unni KK, Beabout JW, Sim FH. Malignant giant cell tumor of the tendon sheaths and joints (malignant pigmented villonodular synovitis). *Am J Surg Pathol*. 1997;21(2):153–63.
36. Dorwart RH, Genant HK, Johnston WH, Morris JM. Pigmented villonodular synovitis of synovial joints: clinical, pathologic, and radiologic features. *AJR Am J Roentgenol*. 1984;143(4):877–85.
37. Miller E, Doria A. Imaging for early assessment of peripheral joints in juvenile idiopathic arthritis. In: Medina LS, Applegate KE, Blackmore CC, editors. *Evidence-based imaging in pediatrics: optimizing imaging in pediatric patient care*. New York: Springer Science+Business Media; 2010.
38. Doria AS, Babyn P. Arthritides and other inflammatory disorders. In: Coley BD, editor. *Caffey's Pediatric Diagnostic Imaging*. Philadelphia: Elsevier; 2013.